Inorganic Chemistry Communications 68 (2016) 17–20

Contents lists available at ScienceDirect

Inorganic Chemistry Communications

journal homepage: www.elsevier.com/locate/inoche

Short communication

Assembly of a 3D chiral Cu(I) metal–organic framework based on 4,5-dicyanoimidazole: CD spectrum, luminescence and selective gas adsorption

Tuo-Ping Hu *, Xiao-Xiao Wang, Bao-Hua Zheng, Xiao-Qing Wang, Xue-Na Hao, Jian-Feng Liu

Department of Chemistry, College of Science, North University of China, Taiyuan 030051, PR China

ARTICLE INFO

Article history:
Received 22 January 2016
Received in revised form 25 March 2016
Accepted 29 March 2016
Available online 4 April 2016

Keywords:
Metal–organic framework
Chiral
Gas adsorption
Photoluminescent

ABSTRACT

One chiral Cu(I) metal–organic framework $\{[Cu(DCI)]\cdot 0.1Cyc\cdot 0.45Nbenz\}_n$ (**1**) (HDCI = 4,5-dicyanoimidazole, Cyc = cyclohexanol, Nbenz = nitrobenzene), was obtained under solvothermal condition. Complex **1** presents a 3D chiral porous framework with 38.2% porosity. The 3D metal–organic framework can be regarded as a PtS net with the vertex symbol of $\{4^2.8^4\}$. The gas adsorption/desorption experiments of complex **1** have been measured at 77 K. Moreover, the CD spectrum and photoluminescent behavior of complex **1** have been studied.

Metal–organic frameworks (MOFs), as a new type of functional materials, have been the subject of growing interest in the past two decades due to their novel topologies and tremendous potential applications in the field of gas adsorption and separation, ion exchange, optics, and heterogeneous catalysis [1–4]. Thousands of MOFs with diverse topologies and excellent properties have been obtained, but chiral MOFs were reported relatively less up to now [5].

To the best of our knowledge, most reported chiral MOFs are derived from the enantiopure organic ligands [6]. There are fewer papers on the chiral MOFs constructed from achiral organic ligands [7]. It's still one tremendous challenge for coordination chemistry researchers to design and synthesize chiral MOFs by using the achiral organic ligands because the processes have not yet been fully understood.

Imidazole and its derivatives have been widely employed in the construction of MOFs due to their versatile bridging modes and tunable backbones by rotating, twisting, or even folding [8–10]. Although the imidazole derivatives have diverse coordination preferences, such as monodentate, bidentate, or bridging fashion, when the cyano groups were added to modify the imidazole compounds, coordination polymers from them were still less reported because the N_{cyano} atoms are weak coordinative sites due to the conjunction of electrons on *p*-orbital with an imidazole ring, and the cyano group is volatile in both acidic and alkaline environments [11].

The achiral 4,5-dicyanoimidazole (HDCI) is one kind of imidazole derivative [12], which was selected to build the chiral MOFs because the $N_{imidazole}$ and N_{cyano} atoms of HDCI ligand can form diverse helical structures by tail-to-tail, tail-to-head, head-to-head, and side-to-side arrangements [12a]. With more helical chains involved, the chiral MOFs can form more easily. Taking into account the above viewpoints, we recently began to assemble the chiral MOFs with HDCI ligand and transitional metal ions and anticipated that the chiral MOFs can feature good gas adsorption and separation.

Yellow block crystals of complex **1** were obtained by solvothermal synthesis from $Cu(ClO_4)_2\cdot 5H_2O$ and HDCI (HDCI = 4,5-dicyanoimidazole) in cyclohexanol/nitrobenzene solution at 100 °C for 3 days. X-ray diffraction analysis reveals that complex **1** crystallizes in a tetragonal system and $P4_12_12$ space group. The asymmetric unit of **1** contains one crystallographically independent Cu^I cation and one DCI^- ligand. Each Cu^I cation is tetra-coordinated and surrounded by four nitrogen atoms from two imidazole N atoms from two DCI^- ligands, and two cyano N atoms from another two DCI^- ligands, leaving a tetrahedral coordination geometry, with the τ_4 parameter at 0.94 (Fig. 1a). A similar Cu(I) coordination geometry has been reported before [13]. The Cu—N bond distances range from 1.949(3) to 2.033(3) Å, and the dihedral angles around Cu^I are in the range of 100.96(12)–116.63(14)°, respectively.

Each DCI^- ligand acts as the μ_4-bridge linking four Cu^I ions through two imidazole N atoms and two cyano N atoms, finally giving a 3D architecture with distinct chains (Fig. 1b). If we consider the imidazole ring as the head, the two cyano groups as the tail, and the one cyano group and a half imidazole ring as the side, those chains can be divided into four categories: the tail-to-tail (A), tail-to-head (B), head-to-head (C), and side-to-side (D). The A-shaped chains are right-handed helices,

---

* Corresponding author.
E-mail address: hutuopingsx@126.com (T.-P. Hu).

http://dx.doi.org/10.1016/j.inoche.2016.03.024
1387-7003/© 2016 Elsevier B.V. All rights reserved.

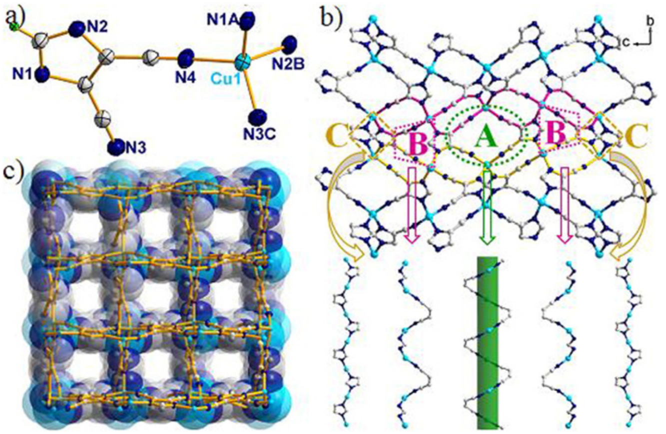

Fig. 1. (a) ORTEP representation of **1** showing the local coordination environment around Cu^{I} center. (b)The 3D framework of complex **1** with distinct chains. (c) The 3D porous framework of complex **1**.

where the width of the helix is calculated to be 5.55 Å and the pitch is 9.36 Å. The B-shaped chains can be regarded as right- and left-handed chiral chains, with the neighboring Cu···Cu distances being 6.04 and 7.26 Å. The C-shaped [Cu(imidazole)]$_n$ zigzag chains are achiral and the imidazole separated Cu···Cu distance is 6.04 Å. The side-to-side D-shaped chain is a loop chain based on the 10-membered ringsand the Cu···Cu distance is 5.49 Å. All the chains joined together to form a 3D porous framework along the *c* direction (Fig. 1c, the square aperture diameter for the channel is 6.04×6.04 Å^2). The porosity for complex **1** calculated by PLATON [14], upon removal of guest solvent molecules, was estimated to be 38.2%.

To better understand the structure of **1**, the topological analysis approach was employed [15]. From the topological point of view, the framework can be simplified to be a binodal (4,4)-connected **PtS** net with the vertex symbol of $\{4^2.8^4\}$ (TD10 = 977) by regarding the Cu^{I} as a 4-connected node (Fig. 2a), featured by the [$4^2.8^2$] + [8^4] tiling ([4^2.8h.8i] + [4^2.8e.8f] + [8b^2.8e.8h] + [8b^2.8f.8i]), with the transitivity of 2464 (Fig. 2b) [16].

Powder X-ray diffraction (XRD) has been used to check the phase purity of the bulky samples in the solid state. For complex **1**, the measured XRD pattern is closely identical to the simulated pattern generated from the result of single-crystal diffraction data by the Mercury program [17], indicative of pure products (Fig. S2, see ESI). The thermogravimetric (TG) analyses on polycrystalline samples of complex **1** were performed in O_2 atmosphere. As shown in Fig. S3, complex **1** shows a weight loss of 3.80% from 45 to 217 °C due to the loss of 0.1 lattice cyclohexanol (calcd: 4.0%). The weight loss of 22.0% between 217 and 337 °C is due to the loss of 0.45 lattice nitrobenzene. The desolvated framework can then stably exist up to a temperature of up to 380 °C. Furthermore, we have also measured the PXRD pattern of the desolvated complex **1a**.

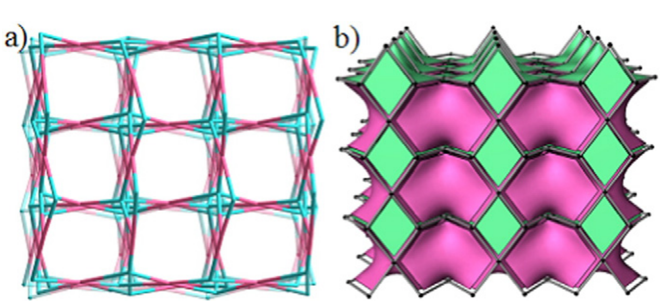

Fig. 2. (a) The binodal (4,4)-connected $\{4^2.8^4\}$-**PtS** net for complex **1**. (b) The tiling featured **PtS** net for complex **1**.

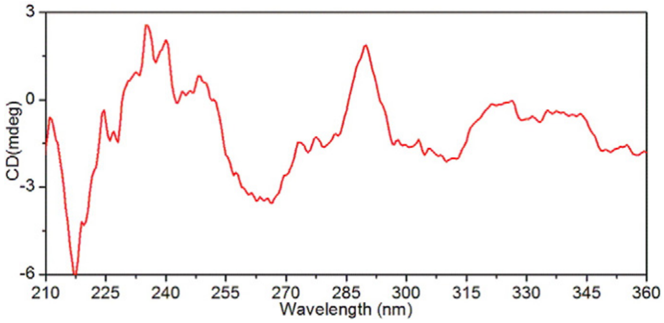

Fig. 3. Solid-state CD spectra of complex **1**.

Circular dichroism (CD) spectroscopy is the most common technique for characterizing the optical activity of chiral materials. The flack factor of **1** is 0.03(3), which indicated that **1** crystallizes in a chiral space group. In order to confirm the chirality of complex **1**, a few crystals were characterized by solid-state circular dichroism (CD) spectroscopy in KCl pellets. As shown in Fig. 3, the CD spectra of complex **1** showed three positive peaks at 240 nm, 290 nm and 330 nm, as well as negative peaks at 217 nm, 264 nm and 305 nm, which may be considered as the signature of helicity for **1** [18].

The photoluminescent behavior of HDCI and complex **1** has been investigated at room temperature, shown in Fig. 4. For the HDCI ligand, the main peak is at 423 nm under 367 nm wavelength excitation, which originates from the π*–π transition of the *p* electrons of the aromatic rings [19]. Complex **1** exhibits luminescent emission peaks at about 452 nm under 330 nm wavelength excitation. Compared with free HDCI, it has a red-shifted (Δ = 29 nm) photoluminescence because of the metal-to-ligand charge transfer transitions, which are similar to some complexes [20]. The CIE chromaticity diagram of complex **1** and HDCI ligand is listed in the insert of Fig. 4. It reveals that the emission colour of complex **1** is blue at CIE chromaticity coordinates (0.19, 0.23).

To confirm the permanent porosity of the framework, gas adsorption measurements of complex **1** were performed. The activated sample **1a** was prepared by exchanging the solvent in the as-synthesized complex **1** with CH_3OH and CH_2Cl_2, followed by evacuation under vacuum. As shown in Fig. S2, the PXRD study shows that the structure of complex **1a** is similar to complex **1**, which indicates the stable framework and permanent porosity of **1a**. The reversible H_2 adsorption isotherms at 77 K show the characteristics of a microporous material with type-I adsorption isotherm behavior (Fig. 5). The H_2 adsorption amounts of complex **1** at 1 bar were about 14.5 cm g^{-1}. Subsequently, we carried out other adsorption experiments on complex **1**. The Brunauer–Emmett–Teller (BET) and Langmuir surface areas of complex **1** are evaluated to be 122.7 and 125.5 m^2 g^{-1}, based on the N_2 adsorption isotherm. As shown in Fig. 5, the N_2, Ar and CO_2 sorption isotherms for

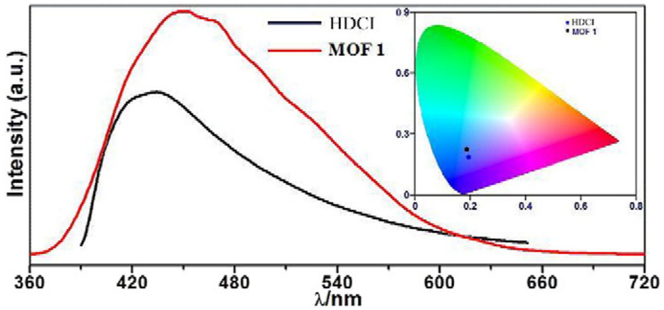

Fig. 4. Solid-state emission spectrum of HDCI ligand and complex **1** at room temperature (insert: the CIE chromaticity diagram of complex **1** and HDCI ligand).